

Polymer Chemistry

Accepted Manuscript



This is an *Accepted Manuscript*, which has been through the Royal Society of Chemistry peer review process and has been accepted for publication.

Accepted Manuscripts are published online shortly after acceptance, before technical editing, formatting and proof reading. Using this free service, authors can make their results available to the community, in citable form, before we publish the edited article. We will replace this *Accepted Manuscript* with the edited and formatted *Advance Article* as soon as it is available.

You can find more information about *Accepted Manuscripts* in the [Information for Authors](#).

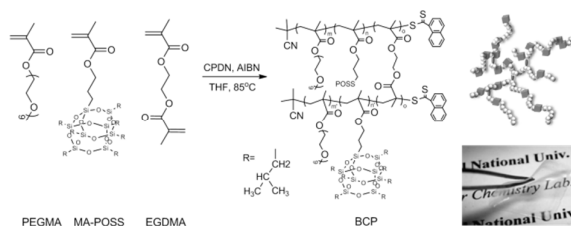
Please note that technical editing may introduce minor changes to the text and/or graphics, which may alter content. The journal's standard [Terms & Conditions](#) and the [Ethical guidelines](#) still apply. In no event shall the Royal Society of Chemistry be held responsible for any errors or omissions in this *Accepted Manuscript* or any consequences arising from the use of any information it contains.

A Table of Contents Entry for

Synthesis and Properties of Organic/Inorganic Hybrid Branched-Graft Copolymers and Their Applications to Solid-State Electrolytes for High-Temperature Lithium-Ion Batteries

Jimin Shim, Dong-Gyun Kim, Jin Hong Lee, Ji Hoon Baik, and Jong-Chan Lee*

* School of Chemical and Biological Engineering and Institute of Chemical Processes, Seoul National University, 599 Gwanak-ro, Gwanak-gu, Seoul 151-742, Republic of Korea. Fax: +82-02-880-8899; Tel: +82-02-880-7070; E-mail: jongchan@snu.ac.kr



A series of organic/inorganic hybrid branched-graft (BCP) copolymers were synthesized via reversible addition fragmentation chain transfer (RAFT) polymerization for applications to solid polymer electrolyte materials in high-temperature lithium-ion batteries.

ARTICLE

Synthesis and Properties of Organic/Inorganic Hybrid Branched-Graft Copolymers and Their Applications to Solid-State Electrolytes for High-Temperature Lithium-Ion Batteries

Cite this: DOI: 10.1039/x0xx00000x

Received 00th January 2012,

Accepted 00th January 2012

DOI: 10.1039/x0xx00000x

www.rsc.org/

Jimin Shim, Dong-Gyun Kim, Jin Hong Lee, Ji Hoon Baik, and Jong-Chan Lee*

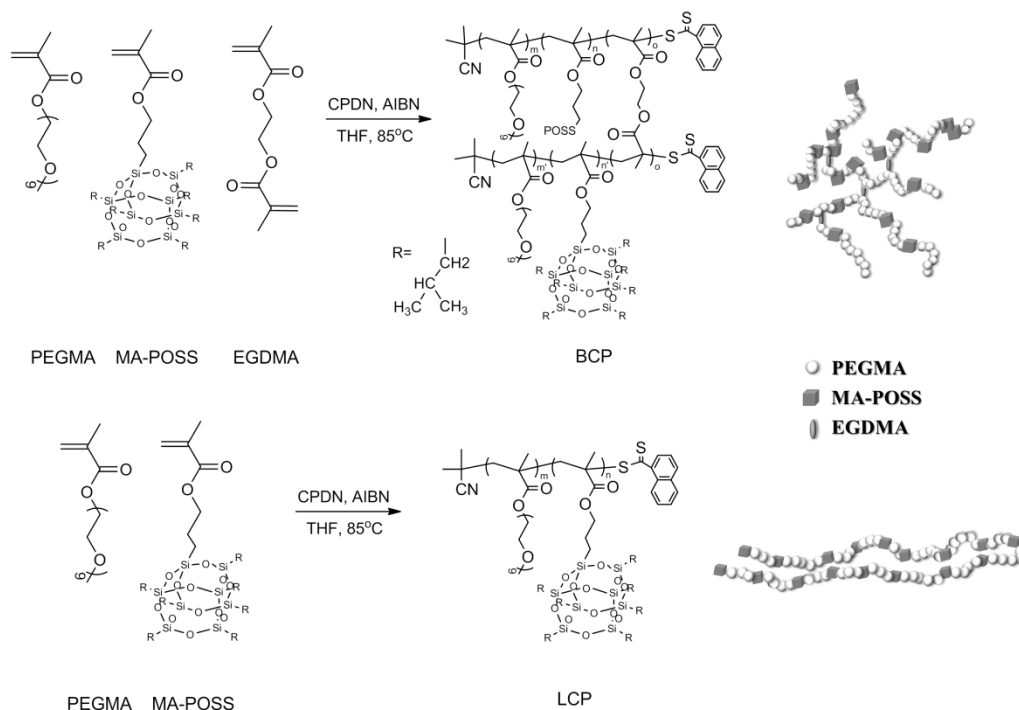
A series of organic/inorganic hybrid branched (BCP) and linear (LCP)-graft copolymers comprising poly(ethylene glycol) methyl ether methacrylate (PEGMA), 3-(3,5,7,9,11,13,15-heptaisobutyl-pentacyclo[9.5.1.1^{3,9}.1^{5,15}.1^{7,13}]octasiloxane-1-yl)propyl methacrylate (MA-POSS), and ethylene glycol dimethacrylate (EGDMA) were synthesized via reversible addition fragmentation chain transfer (RAFT) polymerization for applications to solid polymer electrolyte (SPE) materials in high-temperature lithium-ion batteries. Dimensionally-stable free-standing films were obtained when the MA-POSS contents in BCP and LCP are larger than 21 mol % and maintained its original shape and storage modulus even if temperature increases up to 90 °C. The maximum ionic conductivity value of the BCP electrolyte containing 21 mol % of MA-POSS were 1.6×10^{-4} S/cm at 60 °C and that of the LCP electrolyte containing 21 mol % of MA-POSS were 5.6×10^{-5} S/cm at 60 °C, indicating that the branched-graft copolymer electrolyte has higher ionic conductivity than the linear-graft counterpart, due to the increased chain mobility, as estimated by a smaller T_g value. All-solid-state battery prepared using BCP electrolyte showed reasonable cell performance at 60 °C without causing safety problem, demonstrating a great potential of BCP as SPE materials for high-temperature battery systems.

Introduction

Solid polymer electrolytes (SPEs) for lithium-ion battery applications have attracted great attention in recent years due to the safety issues of the conventional liquid electrolytes.¹⁻³ Organic liquid electrolytes commonly used for most of the commercialized lithium-ion batteries can cause serious safety problems especially at high-temperature due to their high volatility and flammability. In order to widen the applications of lithium-ion batteries to high-temperature such as electric vehicle or surplus electricity storage system at night, the development of high-temperature tolerant SPEs exhibiting good thermal stability, dimensional stability, and high ionic conductivity is required. Linear poly(ethylene oxide) (PEO) has been studied intensively as a matrix for SPEs owing to its ability to conduct lithium ions.⁴⁻⁶ However, it could not be utilized directly for the practical lithium-ion battery applications, due to the low ionic conductivity that originates from the suppressed segmental motions of PEO in the crystalline phase.^{7,8} In order to overcome this shortcoming of the linear PEO-based SPEs, many efforts have been attempted

to develop novel polymer matrices with amorphous state having very small content of the crystalline domains.⁹⁻¹¹ For example, comb-like polymers having short PEG side chains have been used, though they also cannot be used directly for SPEs since they are normally not dimensionally-stable with wax state due to their low glass transition temperatures.^{12,13} To improve the dimensional stability of polymers having short PEG side chains, several approaches using various polymers such as block copolymers¹⁴⁻¹⁶, interpenetrating network polymers^{17,18}, and composite polymers containing nanofillers have been proposed as polymer matrices for the SPEs.^{1,19}

Polyhedral oligomeric silsesquioxane (POSS) is a nano-sized organic/inorganic hybrid material containing a silicon/oxygen framework functionalized with various organic groups at each corner and has been widely used as a nanofiller for polymer composites owing to its superior mechanical strength.²⁰⁻²² POSS also provides additional free volume to the polymer matrix due to the steric effect, resulting in a high chain mobility of the polymers.^{20,23,24} In our previous studies, dimensionally-stable free-standing films were obtained from copolymers having POSS and PEG side groups.^{15,25-27} It was revealed that



Scheme 1 Synthesis of (a) branched (BCP) and (b) linear (LCP)-graft copolymers via RAFT polymerization.

the glass transition temperatures (T_g s) did not increase much with the incorporation of POSS side groups into the polymers having PEG side groups despite the rigidity of the POSS groups. SPEs containing PEG functionalized POSS were also reported by Wunder et al., achieving enhanced ionic conductivity compared to high molecular weight PEO.^{28, 29} Therefore, it could be expected that the POSS side groups in SPEs maintain the chain mobility of PEG segments as well as increase the dimensional stability of the polymers.

Branched polymers have been studied as possible polymer materials for SPEs owing to their amorphous nature, high processability, and the presence of many branch-ends that facilitate lithium-ion conduction.³⁰⁻³⁴ Furthermore, they have larger free volume than the linear counterpart, which results in increased chain mobility.^{35, 36} Although there have been many reports on branched polymers for SPEs, their ionic conductivities have mostly been quite low due to the existence of rigid aromatic groups and their syntheses also require several steps and tedious purification procedures.^{31, 32, 35-41}

In this study, a series of branched-graft copolymers containing POSS side groups for dimensional stability and PEG side groups for lithium-ion conduction were synthesized via one-step RAFT polymerization and applied to SPEs for high-temperature lithium-ion batteries. Linear-graft copolymers with POSS and PEG side groups were also synthesized for comparison. The effects of the POSS content and branched structure on the dimensional stability, thermal properties, and ionic conductivity were systematically investigated. By incorporating the POSS side groups into the wax-state branched poly(poly(ethylene glycol) methyl ether methacrylate) (P(PEGMA)), dimensionally-stable free-standing electrolyte

films exhibiting reasonably high ionic conductivity could be prepared. The branched-graft copolymer electrolytes exhibited higher ionic conductivity than the linear-graft copolymer electrolytes when they had the same monomer composition.

Experimental Section

Materials

2,2'-Azobis(isobutyronitrile) (AIBN, Junsei) was recrystallized from ethanol prior to use. Poly(ethylene glycol) methyl ether methacrylate (PEGMA, average $M_n = 475 \text{ g mol}^{-1}$) and ethylene glycol dimethylacrylate (EGDMA) was purchased from Aldrich and passed through an alumina column prior to polymerization. Methacrylisobutyl POSS[®] (3-(3,5,7,9,11,13,15-heptaisobutyl-pentacyclo[9.5.1.1^{3,9}.1^{5,15}.1^{7,13}]octasiloxane-1-yl)propyl methacrylate, MA-POSS) was purchased from Hybrid Plastics (product no. MA0702) and used as received. Tetrahydrofuran (THF) was freshly distilled from sodium/benzophenone under a nitrogen atmosphere. Lithium bis(trifluoromethane sulfonyl)imide (LiTFSI, >98%, TCI) was dried under high vacuum at 130 °C for 24 h and subsequently placed in an argon filled glove box. The chain transfer agent (CTA), 2-cyanoprop-2-yl-1-dithionaphthalate (CPDN), was synthesized as previously described.⁴²⁻⁴⁴ All other reagents and solvents were obtained from reliable commercial sources and used as received.

Synthesis of branched-graft poly(poly(ethylene glycol) methyl ether methacrylate-*r*-methacrylisobutyl-POSS) (BCP)

Branched-graft poly(poly(ethylene glycol) methyl ether methacrylate-*r*-methacrylisobutyl-POSS) is abbreviated to BCP.

Table 1 Synthesis results of the series of linear and branched-graft copolymers with different comonomers feeding ratios

Samples	Composition (PEGMA : MA-POSS) ^a			$M_w^{b(c)}$	$M_w^{d(e)}$	M_w^b / M_w^d	State ^f
	Feed [mol%]	In polymer [mol%]	In polymer [wt%]	[10 ⁻³ , RI]	[10 ⁻³ , MALLS]		
Linear P(PEGMA)	100 : 0	100 : 0	100 : 0	2.4 (1.28)	50.8 (1.03)	0.05	Wax
Branched P(PEGMA)	100 : 0	100 : 0	100 : 0	4.8 (1.50)	177.3 (1.15)	0.03	Wax
BCP9	89 : 11	91 : 9	84 : 16	5.7 (1.53)	152.8 (1.04)	0.04	Sticky film
LCP21	77 : 23	79 : 21	65 : 35	16.4 (1.17)	128.4 (1.35)	0.13	Free-standing film
BCP21	77 : 23	79 : 21	65 : 35	16.2 (1.31)	139.6 (1.08)	0.12	Free-standing film
LCP29	68 : 32	71 : 29	56 : 44	16.6 (1.43)	117.8 (1.15)	0.14	Free-standing film
BCP30	68 : 32	70 : 30	54 : 46	12.3 (1.68)	140.6 (1.18)	0.09	Free-standing film
LCP35	62 : 38	65 : 35	51 : 49	23.6 (1.23)	163.9 (1.01)	0.14	Free-standing film
BCP36	62 : 38	64 : 36	47 : 53	25.8 (1.30)	341.8 (1.07)	0.08	Free-standing film

^a Determined by ¹H NMR. ^b Determined by GPC using refractive index (RI) detector, calibrated with linear polystyrene standards (THF). ^c PDI values determined by GPC using RI detector (THF). ^d Determined by GPC using multi-angle laser light scattering (MALLS) detector (THF). ^e PDI values determined by GPC using MALLS detector (THF). ^f State after cast onto Teflon plate at room temperature.

Schematic illustration of the synthesis procedures of BCP and LCP is presented in Scheme 1. BCP21 containing 21 mol % of MA-POSS and 79 mol % of PEGMA monomeric units were synthesized via RAFT polymerization as follows. PEGMA (5.4 g, 11.3 mmol), MA-POSS (3.02 g, 3.0 mmol), EGDMA (0.045 g, 0.023 mmol), CPDN (0.031 g, 0.11 mmol), and AIBN (0.006 g, 0.034 mmol) were dissolved in 14 mL of distilled THF and the resultant solution was added to a 100 mL Schlenk flask equipped with a magnetic stirring bar and a condenser. The solution was degassed by three consecutive freeze-pump-thaw cycles to remove oxygen and the reaction was performed in an oil bath thermostated at 85 °C for 21 h under nitrogen atmosphere. After the flask was removed from the oil bath, it was exposed to air and diluted with THF to quench the reaction. The unreacted monomers were removed by precipitation in hexane three times. After dried under vacuum at room temperature several days, pink rubbery solid product was obtained with 68 % yield. Other BCPs were also prepared from the same synthetic procedure with different monomer feeding ratios as shown in Table 1. ¹H NMR [300 MHz, CDCl₃, δ (ppm), TMS ref] of BCP21: 4.08 (CH₂-O-C(O)), 3.48-3.85 (CH₂-CH₂-O), 3.38 (CH₃-O), 1.85 (isobutyl, CH), 1.53-2.05 (methacrylate backbone, CH₂-C(CH₃)(C=O)), 0.95 (isobutyl, CH₃), 0.6 (isobutyl, CH₂), 0.78-1.11 (methacrylate backbone, CH₂-C(CH₃)(C=O)).

Synthesis of linear-graft poly(poly(ethylene glycol) methyl ether methacrylate-*r*-methacrylisobutyl-POSS) (LCP)

Linear-graft poly(poly(ethylene glycol) methyl ether methacrylate-*r*-methacrylisobutyl-POSS) is abbreviated to LCP. LCP21 containing 21 mol % of MA-POSS and 79 mol % of PEGMA monomeric units were synthesized via RAFT polymerization as follows. PEGMA (5.4 g, 11.3 mmol), MA-

POSS (3.02 g, 3.0 mmol), CPDN (0.031 g, 0.11 mmol), and AIBN (0.006 g, 0.034 mmol) were dissolved in 14 mL of distilled THF and the resultant solution was added to a 100 mL Schlenk flask equipped with a magnetic stirring bar and a condenser. The solution was degassed by three consecutive freeze-pump-thaw cycles to remove oxygen and the reaction was performed in an oil bath thermostated at 85 °C for 21 h under nitrogen atmosphere. After the flask was removed from the oil bath, it was exposed to air and diluted with THF to quench the reaction. The unreacted monomers were removed by precipitation in hexane three times. After dried under vacuum at room temperature several days, pink rubbery solid product was obtained with 71 % yield. Other LCPs were also prepared from the same synthetic procedure with different monomer feeding ratios (Table 1). ¹H NMR [300 MHz, CDCl₃, δ (ppm), TMS ref] of LCP21: 4.1 (CH₂-O-C(O)), 3.48-3.85 (CH₂-CH₂-O), 3.38 (CH₃-O), 1.85 (isobutyl, CH), 1.53-2.05 (methacrylate backbone, CH₂-C(CH₃)(C=O)), 0.95 (isobutyl, CH₃), 0.6 (isobutyl, CH₂), 0.78-1.11 (methacrylate backbone, CH₂-C(CH₃)(C=O)).

Preparation of solid polymer electrolytes (SPEs)

The solid polymer electrolytes containing LiTFSI and polymers in various blend compositions were prepared by a solution casting technique. Doping levels are defined as the ratio of the number of lithium cations (Li⁺) to that of ethylene oxide (EO) repeating unit in the polymers ([Li]/[EO]). 0.1 g of polymers and the given amounts of LiTFSI were dissolved in 0.5 mL of THF and homogeneous solution was obtained. After that, the solution was cast onto a Teflon plate (2 x 2 cm²) and dried at room temperature for overnight. Subsequently, it was further dried under high vacuum at room temperature for 24 h. Finally, the film was peeled off from the Teflon plate and the resultant

film was placed in a high vacuum condition for a week at 80 °C prior to measure the ionic conductivities of the solid polymer electrolytes. The thickness of the films measured by a micrometer (Mitutoyo, 293-330 IP 65 water resistant) was in the range of 200-300 μm .

Cell fabrication and electrochemical characterization

The electrochemical stability of BCP21 was evaluated using linear sweep voltammetry (LSV). The cell was assembled by sandwiching BCP21 electrolyte between stainless steel (working electrode) and lithium metal (reference electrode) in 2032 coin cell. The cell was swept in the potential range from 1 V to 7 V (versus Li/Li^+) at scan rate of 1 mV/s at 60 °C. Charge/discharge test of all-solid-state lithium-ion battery was performed at cutoff voltages of 2.0 ~ 3.8 V versus Li/Li^+ at 60 °C with current density of 0.1 C. V_2O_5 (60 wt%) was used as cathode active material and dispersed in N-methyl-2-pyrrolidone (NMP) with carbon black (20 wt%) and PVDF (20 wt%). The resultant slurry was deposited and cast onto Aluminium current collector using doctor blade. The residual NMP was completely dried under vacuum condition at 100 °C for 1 day. The obtained cathode sheet, lithium metal, and solid polymer electrolyte (SPE) were punched into disk and assembled together in 2032 coin cell to form $\text{Li}/\text{SPE}(\text{BCP21})/\text{V}_2\text{O}_5$ cell. All components were prepared in argon filled glove box ($\text{H}_2\text{O} < 0.5$ ppm, $\text{O}_2 < 0.5$ ppm).

Characterization

^1H nuclear magnetic resonance (NMR) spectra were recorded on an AscendTM 400 spectrometer (300 MHz) using CDCl_3 (Cambridge Isotope Laboratories) as the solvent at room temperature with tetramethylsilane (TMS) as a reference. ^{13}C and ^{29}Si NMR spectra were recorded on JeolJNM-LA400 spectrometer (400 MHz) using CDCl_3 (Cambridge Isotope Laboratories) as the solvent at room temperature. Molecular weights (M_n , M_w) and polydispersity index (PDI) were analyzed by gel permeation chromatography (GPC). Relative molecular weight was measured by GPC equipped with a Waters 515 HPLC pump and three columns including PLgel 5.0 μm guard, MIXED-C, and MIXED-D from Polymer Laboratories in series with a Viscotek LR125 laser refractometer. The system with a refractive index (RI) detector was calibrated using polystyrene standards from Polymer Laboratories. The resulting data was analyzed using the Omniseq software. Absolute molecular weights of polymers were analyzed using a Waters 515 HPLC pump equipped with three columns including PLgel 5.0 μm guard, MIXED-C, and MIXED-D from Polymer Laboratories in series with a Wyatt Technology MiniDAWNTM triple-angle light scattering detector and a Wyatt Technology Optilab DSP interferometric refractometer. HPLC grade THF (J. T. Baker) was used as the eluent at a flow rate of 1.0 mL min^{-1} at 35 °C. The thermal transition temperatures of the polymers were examined by differential scanning calorimetry (DSC) using TA Instruments DSC-Q1000 under a nitrogen atmosphere. Samples with a typical mass of 3-7 mg were encapsulated in sealed aluminium pans. The samples were first heated to 150 °C and

then quenched to -80 °C. This was followed by a second heating scan from -80 °C to 150 °C at a heating rate of 10 °C min^{-1} . The thermal stability of the polymers was investigated by thermogravimetric analysis (TGA) using TA Instruments TGA Q-5000IR under nitrogen atmosphere. The samples were maintained at 130 °C for 10 min to remove residual water molecules, and then heated to 700 °C at a heating rate of 10 °C min^{-1} . Transmission electron microscopy (TEM) was performed on a LIBRA 120 with an accelerating voltage of 120 kV. TEM specimens were prepared by drop casting of 1 wt% polymer solutions in THF on carbon-coated copper grid. Temperature-resolved rheological measurement was carried out using an rheometer (Advanced Rheometric Expansion System, ARES) in the linear viscoelastic region with 0.1 rad s^{-1} of frequency at 1 °C min^{-1} ramp. Shear viscosity was also measured using ARES rheometer. Each sample was subjected to a shear rate of 10 Hz for 120 seconds at 30 °C. The average viscosity value was calculated and used as x-axis of Walden plot. The ionic conductivity of the SPEs was analyzed by complex impedance spectroscopy between 10 to 80 °C under dry nitrogen condition using Zahner Elektrik IM6 apparatus in the frequency range of 0.1 Hz to 1 MHz and an applied voltage of 10 mV. The real part of the impedance at the minimum of imaginary part was used as the resistance to calculate the conductivity of the SPEs. The samples for the measurements were prepared by sandwiching the SPEs between two stainless-steel electrodes. Each sample was allowed to equilibrate for 30 min at each temperature prior to taking measurements. The ionic conductivity (σ) was calculated from the electrolyte resistance (R) obtained from the impedance spectrum, the electrolyte thickness (d) and the area of the electrode (A) using the following equation, $\sigma = (l/R) \times (d/A)$. Electrochemical stability was evaluated by linear sweep voltammetry (LSV) using a potentiostat (VMP3, Biologics) at 60 °C at scan rate of 1 mV/s. Charge/discharge test of all-solid-state lithium-ion battery was performed with a WBCS3000 battery cyler (WonATech) at 60 °C.

Results and discussion

Synthesis of organic/inorganic hybrid branched and linear-graft copolymers

A series of organic/inorganic hybrid branched-graft copolymers (BCPs) was synthesized via RAFT polymerization. Since RAFT polymerization follows the pseudo-living polymerization mechanism, it has many advantages over the free radical polymerization regarding the control of polymer structures, molecular weights, and polydispersity.⁴⁵⁻⁴⁹ For example, when diacrylate monomers are included in the polymerization systems, well-defined branched polymers with low PDI values could be prepared via RAFT polymerization without any gelation, whereas cross-linked polymers are normally obtained through the free radical polymerization.^{50, 51}

The synthetic procedures of BCPs with PEGMA and MA-POSS monomeric units are illustrated in Scheme 1. PEGMA

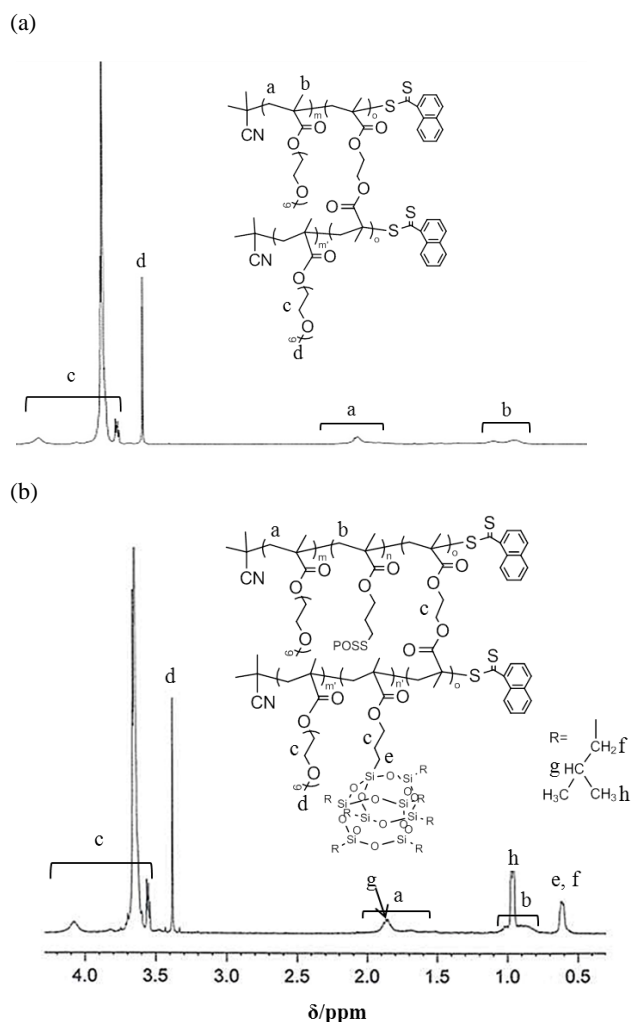


Fig. 1 ^1H NMR spectrum of (a) branched P(PEGMA) and (b) BCP21.

and MA-POSS are comonomers and EGDMA acts as a branching agent to generate bridges between linear chains. MA-POSS was incorporated in order to enhance the dimensional stability of polymers because P(PEGMA) homopolymer without any POSS moieties was found to be in a waxy state. CPDN was chosen as a chain transfer agent (CTA) to mediate the RAFT polymerization in this study because it has been widely used as an effective CTA to prepare polymers with low PDI from the living radical polymerization of methacrylate monomers.⁵² The feed ratio of PEGMA and/or MA-POSS : EGDMA : CPDN : AIBN was fixed to 100 : 2 : 1 : 0.3. The molar ratio of EGDMA to CPDN was determined as 2 : 1 in order to prepare branched polymers without any gelation because gelation occurs during the polymerization when the ratio of EGDMA/CPDN is larger than 3. Linear-graft copolymers (LCPs) were also prepared using only two monomers, PEGMA and/or MA-POSS, without a branching agent in order to investigate the structural effects on the properties of polymers.

The structure of polymers was confirmed by ^1H NMR analysis, as shown in Fig. 1. The signals c and d at 3.48-4.21 ppm and 3.38 ppm are assigned to the $\text{CH}_2\text{-CH}_2\text{-O}$ and terminal $\text{CH}_3\text{-O}$ of PEG side groups, respectively. Signals a and b at 1.53-2.05 ppm and 0.78-1.11 ppm can be assigned to the methylene and methyl protons of the poly(methacrylate) backbone, respectively, although these signals could not be clearly verified due to their low intensity. The presence of protons from MA-POSS in BCP21 was also clearly confirmed. The peaks observed at 0.6 ppm (signals e and f) are assigned to the methylene protons of MA-POSS. The protons from isobutyl groups of MA-POSS are observed at 1.85 ppm (signal g) and 0.95 ppm (signal h). The compositions of monomers in the copolymers were calculated from the following equation (1):

$$\text{MA-POSS Content (mol \%)} = \frac{(I_{e+f}/16)}{[(I_d/3) + (I_{e+f}/16)]} \times 100 \quad (1)$$

where I_d is the integral value of the signal d at 3.38 ppm corresponding to the methyl protons of PEGMA moieties and I_{e+f} is the integral value of signals e and f at 0.6 ppm, corresponding to the methylene protons of MA-POSS moieties. Additionally, the presence of POSS moieties in BCP21 was also verified by ^{29}Si NMR and ^{13}C NMR analysis (Fig. S1 and S2, respectively in Supporting Information). In ^{29}Si NMR spectrum, there are two resonance peaks due to different proximity of silicon atoms to the methacryl side chains. These two peaks at -67.2 ppm and -67.4 ppm correspond to the isobutyl substituted silicon.⁵³ In ^{13}C NMR spectrum, signals in 70-80 ppm are assigned to $\text{CH}_2\text{-CH}_2\text{-O}$ units, and signal from terminal $\text{CH}_3\text{-O}$ of PEG side groups is shown at 59.2 ppm. Signals from isobutyl groups attached to the silicon of POSS and carbons in polymer backbone are clearly observed at 20-30 ppm.

Although the branching points could not be elucidated from the ^1H NMR spectra, the presence of branching in the copolymers could be estimated by the differences in their absolute and relative molecular weights (M_w MALLS and M_w RI, respectively) as shown in Table 1. It is known that branched-graft copolymers have smaller hydrodynamic volume than that of the linear counterparts.^{35, 54} M_w RI/ M_w MALLS values of BCPs are always smaller than those of the corresponding LCPs, indicating that BCPs have some branching points in their structures. Furthermore, BCPs have higher absolute molecular weights than the corresponding LCPs when they have the same monomer composition because EGDMA generates bridges between the linear polymer chains.

The MA-POSS content in the polymers was controlled to be in the range of 9 - 36 mol % in this study. Flexible free-standing films could be prepared from the copolymers when MA-POSS content was in the range of 21 - 40 mol %. Although we tried to synthesize BCPs having larger MA-POSS content than 40 mol %, it was difficult to purify the copolymers due to their amphiphilic properties. For instance, copolymers having MA-POSS content larger than 40 mol % are soluble in nonpolar solvents such as hexane and ether as well as in polar solvents

such as methanol, and then the resulting copolymers cannot be separated easily from the monomers.

Thermal properties

BCP21, BCP30, BCP36, and LCP21 were chosen to evaluate the effects of the POSS content and the polymer structures on the thermal properties and ionic conductivities because dimensionally-stable free-standing films could be prepared from them and the purpose of this study is the possible application of the newly synthesized copolymers for SPE applications.

Fig. 2 shows the DSC thermograms of the four organic/inorganic hybrid copolymers with MA-POSS moieties and branched P(PEGMA) without MA-POSS moieties. The branched P(PEGMA) shows a distinct melting transition peak (T_m) at -3.5 °C, indicating that the branched P(PEGMA) has a semicrystalline phase, because it has crystalline PEG side chains.⁵⁵ In contrast, the melting transition peak is not observed for the copolymers with MA-POSS moieties, because the bulky POSS side groups suppress the crystallization of PEG side chains.⁵⁶ The copolymers having MA-POSS moieties show two glass transition temperatures at around -60 and 80 °C, respectively. The lower and higher ones are originated from the chain motions from PEGMA and MA-POSS segments in the copolymers, respectively.^{15, 24}

Although the rigidity of POSS can suppress the mobility of polymer segments due to the rigid nature of POSS, the large volume of POSS can also provide interchain spacing and free volume of polymers to reduce the rotational energy barrier.⁵⁶⁻⁵⁸ Moreover, flexible linear side chains such as PEG side groups can work as a plasticizer when they do not have ordered structures, thereby decreasing the T_g .⁵⁹ Since T_g of copolymers could be affected by both steric barrier and free volume effect of the POSS and PEG side groups, it could not be easily explained simply by the content of each monomeric units. To further study the effect of POSS moieties on the glass transition behavior of BCPs, BCP13 having 13 mol % of POSS monomer

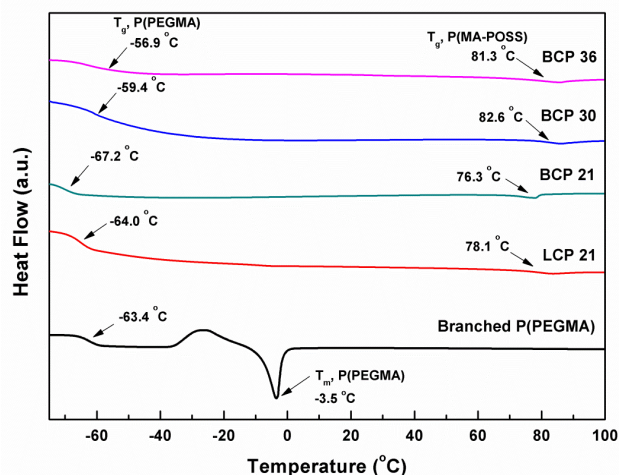


Fig. 2 DSC thermograms of LCP21 and BCPs.

was intentionally synthesized and its T_g of P(PEGMA) segment was found to be -70.1 °C which is lower than those of branched P(PEGMA) (-63.4 °C) and other BCPs. As shown in Supporting Information (Fig. S3), T_g of P(PEGMA) segments in BCP decreases with the increase of the POSS content to 13 mol %, then further increases when the POSS content is larger than about 13 mol %. However, when the POSS content is less than 30 mol %, the T_g is even smaller than that of P(PEGMA) because the POSS groups can provide considerable free volume offsetting the rigid nature of POSS. In other words, the flexibility of ion-conducting PEG side chains can be maintained when the POSS content is less than 30 mol %.

Meanwhile, T_g of P(PEGMA) segments in BCP21 is smaller than that of the LCP21, indicating that the chain mobility of the branched-graft polymers is larger than that of the linear-graft polymers when they have the same monomer composition. The larger chain mobility of BCP21 than that of the LCP21 can be ascribed to the larger free volume of branched-graft polymers than that of the linear counterparts. Similarly, larger chain mobility and smaller T_g values of branched polymers over the

Table 2 Thermal properties of the linear and branched-graft copolymers

Samples	T_g (°C) ^a	T_g (°C) ^b	T_g (°C) ^c	$T_d, 5\%$ (°C) ^d	Char yield (%) ^e
Branched P(PEGMA)	-63.4	-41.2	-	289	0.1
LCP21	-64.0	-38.5	78.1	232	0.9
LCP29	-56.7	-36.3	85.2	220	1.0
LCP35	-53.3	-33.2	85.9	212	1.8
BCP21	-67.2	-40.0	76.3	277	0.2
BCP30	-59.4	-38.2	82.6	262	1.1
BCP36	-56.9	-35.6	81.3	244	1.9

^a T_g of P(PEGMA) segments in polymers. ^b T_g of P(PEGMA) segments in polymers containing LiTFSI ([Li]/[EO] = 0.07). ^c T_g of P(MA-POSS) segments in polymers. ^e The char yield at 700 °C.

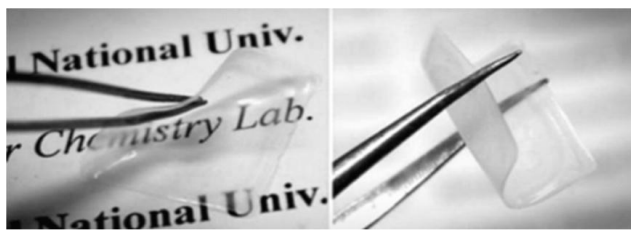


Fig. 3 BCP21 electrolyte containing LiTFSI ([Li]/[EO] = 0.03).

linear polymers were also reported by others.^{35, 36}

The degradation temperatures at 5 % weight loss ($T_{d, 5\%}$) of the polymers are summarized in Table 2. The thermal decomposition of the polymers occurred above 200 °C. $T_{d, 5\%}$ values of the polymers decrease with increasing MA-POSS content, because the isobutyl vertex groups of the POSS moieties decompose at lower temperature.²⁴ Furthermore, $T_{d, 5\%}$ s of BCP21 and LCP21 are 277 °C and 232 °C, respectively, suggesting that the branched-graft polymer has better thermal stability than the corresponding linear-graft polymer.⁶⁰

SPE films containing various LiTFSI concentrations ([Li]/[EO] = 0.03 – 0.11) were prepared from BCPs and LCP21 by solution casting technique. The prepared SPEs were flexible and transparent free-standing films as shown in Fig. 3. These copolymers having MA-POSS moieties show dimensional stability as films at room temperature, because the glass transition temperatures of the MA-POSS segments are much higher than room temperature. Also, the presence of nanoscale-domain of the MA-POSS moieties was confirmed by TEM micrographs as shown in Fig. 4. Although the polymers have random structure with PEG and POSS moieties, some phase separation could happen in the copolymer.^{21, 61-63} Dark spots corresponding to the POSS-rich domain could be observed without additional staining processes, since the silicon in the POSS has high electron density.⁶⁴ The dark spots are randomly distributed in the matrix, and the size of the POSS-rich domain

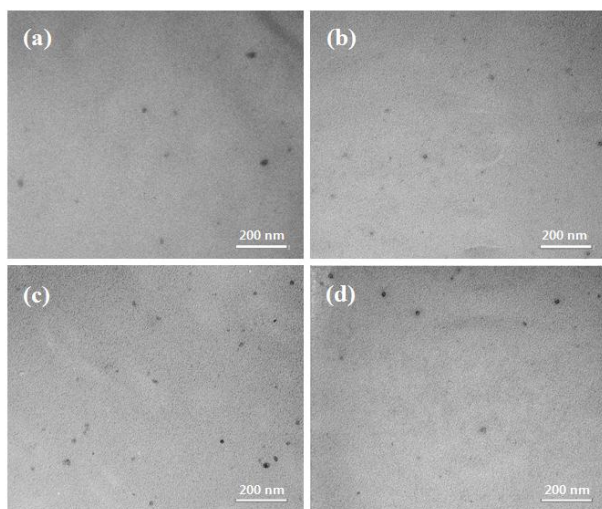


Fig. 4 TEM micrographs of (a) LCP21, (b) BCP21, (c) BCP30, and (d) BCP36.

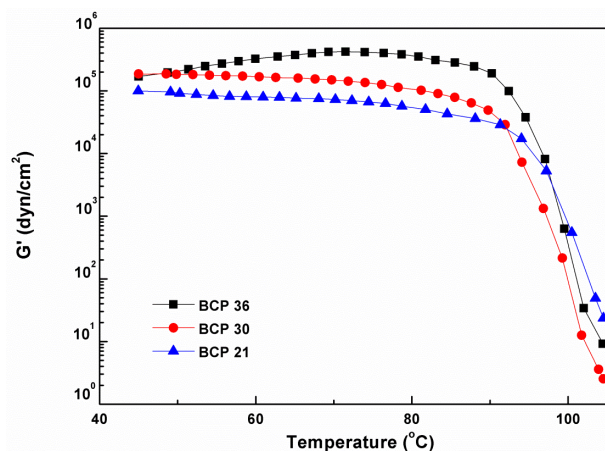


Fig. 5 Temperature-resolved rheological behaviors of BCP21, BCP30, and BCP36 electrolyte films ([Li]/[EO] = 0.07) in the linear viscoelastic region with 0.1 rad s⁻¹ of frequency at 1 °C min⁻¹ ramp.

is around 20 nm, indicating that the POSS rich domain was formed through the aggregation of 10-15 blocks of POSS cages, because the approximate diameter of single POSS cage is about 1.5 nm.

Fig. 5 presents the temperature-resolved rheological behaviors of the BCP electrolyte films ([Li]/[EO] = 0.07). It was revealed that the storage modulus (G') values were maintained until the temperature reaches the T_g of P(MA-POSS) segments, even though the T_g of the ion-conducting phase is quite low (around -60 °C). This result suggests that the formation of dimensionally-stable free-standing films is mainly attributed to the existence of the POSS-rich domain. Owing to this fact, the dimensional stability of the BCP electrolyte films could be maintained as its original shape even if temperature increases up to 90 °C. Then we don't need a separator in the assembly of lithium-ion battery because the inter-electrode distance could be maintained using the solid-state BCP electrolyte even at the elevated temperature. Therefore, BCP21 can be utilized as SPE for lithium-ion batteries operated at high-temperature. It is noteworthy that random copolymer prepared by simple one-step random copolymerization without any block copolymer structure exhibits good dimensional stability. Furthermore, the G' value increases as the POSS content increases in the polymers, suggesting that the POSS moieties in the polymers definitely enhance the dimensional stability of the SPEs.^{65, 66}

Ionic conductivity

Fig. 6 shows the ionic conductivities of branched P(PEGMA), LCP21, and BCP electrolytes containing LiTFSI with various concentrations at 30 °C. According to equation (2), the ionic conductivity is related to the number of charge carriers and their mobility; n is the number of charge carriers, q is the charge on each charge carriers, and μ is the mobility of charge carriers.⁶⁷

$$\sigma = \sum n q \mu \quad (2)$$

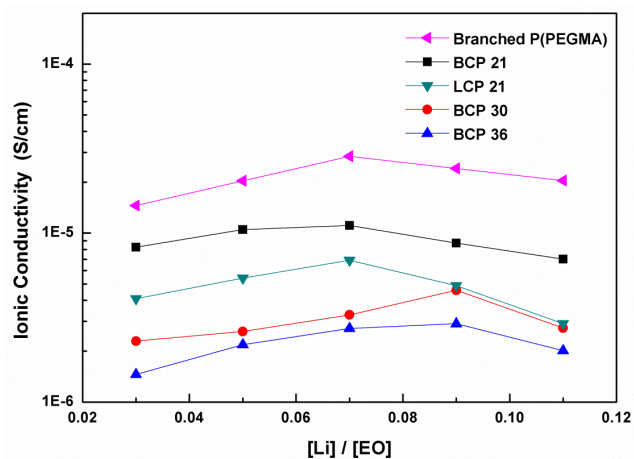


Fig. 6 Ionic conductivities of LCP21 and BCPs containing LiTFSI with various concentrations at 30 °C.

Although the ionic conductivity (σ) is expected to increase linearly as the lithium salt concentration (n) increases, the ionic conductivity does not increase continuously with increasing lithium salt concentration. It reaches a maximum value at a certain ratio of $[Li]/[EO]$, followed by a decrease with a further increase in lithium salt content. The optimum salt concentrations were found at $[Li]/[EO]$ of 0.07 for branched P(PEGMA), BCP21, and LCP21, and at 0.09 for BCP30 and BCP36. This decrease could be attributed to two contributions. First, as the lithium salt concentration increases in the SPEs, the formation of associated ionic species such as contact ion pairs or ion aggregates also increases, thereby decreasing the number of effective charge carriers.⁶⁸ Second, the polymer chain mobility gradually decreases with increasing lithium salt concentration as estimated by the increase in T_g values as shown in Fig. 7. This is ascribed to the increase in intermolecular or intramolecular interactions between the oxygen of the PEG moieties and the lithium cations with

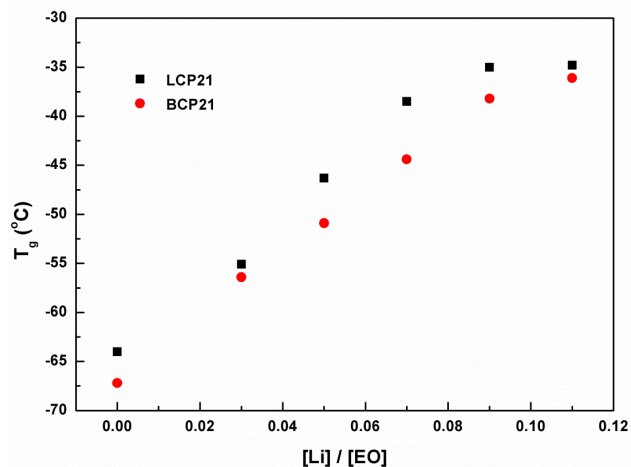


Fig. 7 Glass transition temperatures of P(PEGMA) segments in LCP21 and BCP21 with various LiTFSI concentrations.

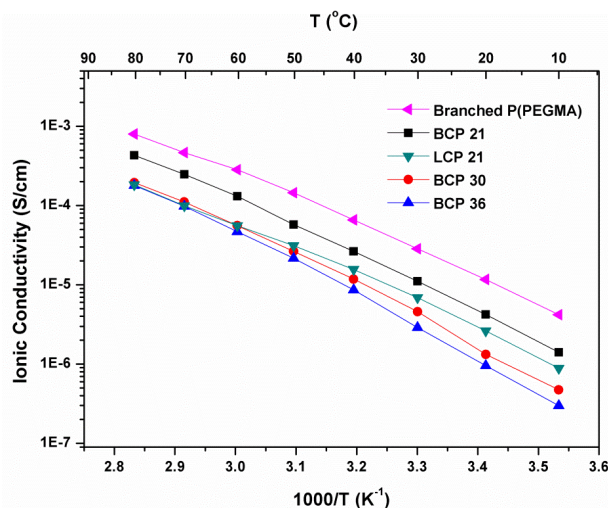


Fig. 8 Temperature dependence of ionic conductivities of LCP21 and BCPs, where each electrolyte contains same lithium salt concentration ($[Li]/[EO] = 0.07$).

increasing lithium salt concentration.⁶⁹ Therefore, the number of effective charge carriers and the mobility of polymer segments decrease with increasing lithium salt concentration, resulting in a decrease in the ionic conductivity of the polymer electrolytes with larger amount of lithium salts. The decrease in ionic conductivity of SPEs at high salt concentrations was also observed for other polyether-based polymer electrolytes.⁷⁰ To further study the conductivity behavior of the electrolytes, molar conductivity as a function of square root of LiTFSI concentration for each electrolyte and Walden plot (molar conductivity vs. shear fluidity (viscosity⁻¹)) of BCP21 were depicted as shown in Supporting Information (Fig. S4). The molar conductivity firstly decreases until the salt concentration reaches to certain ratio due to formation of ion pairing, and then increases to reach the maximum conductivity due to formation of ion triplets and re-dissociation effect. At high LiTFSI concentration, the conductivity decreases again due to further increase of T_g and viscosity. In addition to the T_g of the polymer electrolytes, viscosity has been known to another very important factor affecting the ionic conductivity.⁷¹ Walden plot in the Supporting Information (Fig. S4(b)) shows the relationship between viscosity and ionic conductivity very well; the increase of viscosity with LiTFSI concentration decreases the molar conductivity.

Fig. 8 shows the temperature dependence of ionic conductivities of branched P(PEGMA), LCP21, and BCP electrolytes, where each electrolyte has the same lithium salt concentration ($[Li]/[EO] = 0.07$). It was revealed that the electrolytes with smaller POSS content exhibit higher ionic conductivities. BCP21 electrolyte exhibits maximum ionic conductivity over the entire temperature ranges among the SPEs. The ionic conductivity of BCP21 (1.6×10^{-4} S/cm) is about three times higher than that of BCP36 (4.7×10^{-5} S/cm) at 60 °C. The lithium-ion conduction in SPEs occurs through long-range migration of lithium-ions by the exchange of solvation sites, as the PEG side groups have mobility in the polymer matrix at temperatures above T_g .²⁸ As the POSS

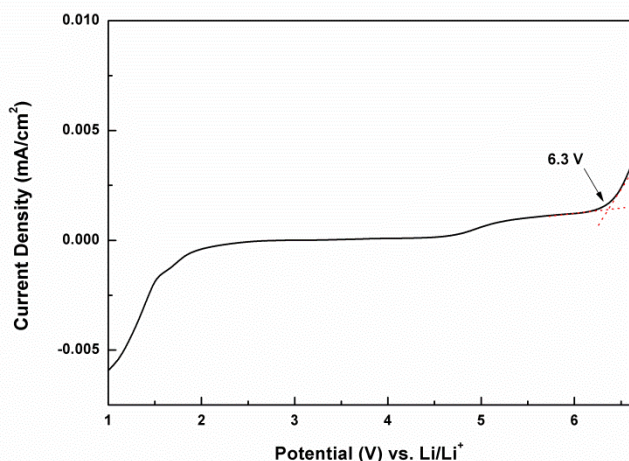


Fig. 9 Linear sweep voltammogram of BCP21 ([Li]/[EO] = 0.07) at 60 °C with scan rate of 1 mV/s.

content in the polymer matrix increases, the mobility of the polymer decreases, because the bulky POSS groups can work as a steric barrier, as estimated by the increase of T_g values of ion-conducting PEG segments in the electrolytes (Table 2). Therefore, the polymer electrolytes containing smaller POSS content have larger chain mobility and exhibit higher ionic conductivities. In addition, the lithium ion content of the electrolytes also affects the ionic conductivity. The polymer electrolytes containing smaller POSS content have larger PEG content, indicating that more lithium ions exist in the SPEs with smaller POSS content when the lithium salt concentrations are same ([Li]/[EO] = 0.07). Meanwhile, BCP21 electrolyte exhibits higher ionic conductivity than the LCP21 electrolyte. This result is ascribed to the larger chain mobility of the branched-graft polymer compared to that of the linear counterpart, as estimated by the lower T_g value of ion-conducting PEG segments originating from the larger free volume.^{35, 36}

Electrochemical stability and all-solid-state cell performance

In order to operate the lithium-ion battery at broad potential window, the electrochemical stability of electrolyte is considered to be crucial factor. The electrochemical stability of BCP21 was evaluated by using linear sweep voltammetry with SS (Stainless steel)/BCP21/Li coin cell at 60 °C as shown in Fig. 9. The current density is almost constant until the applied voltage swept to about 6.3 V. The abrupt rise of current at about 6.3 V corresponds to the electrochemical oxidative degradation of electrolyte. However, BCP21 is still electrochemically stable within the operation voltage range of V_2O_5 cathode as well as other higher voltage class cathode materials. This potential window is much wider than those of linear PEO-based electrolytes. Moreover, the electrochemical window of BCP21 is larger than that of organic liquid electrolytes (~ 4.5 V). Therefore, BCP21 can be applied to high-voltage battery systems over a wide temperature range.

Charge/discharge test of all-solid-state Li/BCP21/ V_2O_5 cell was performed at 60 °C cycled at 0.1 C rate (Fig. 10). Quite

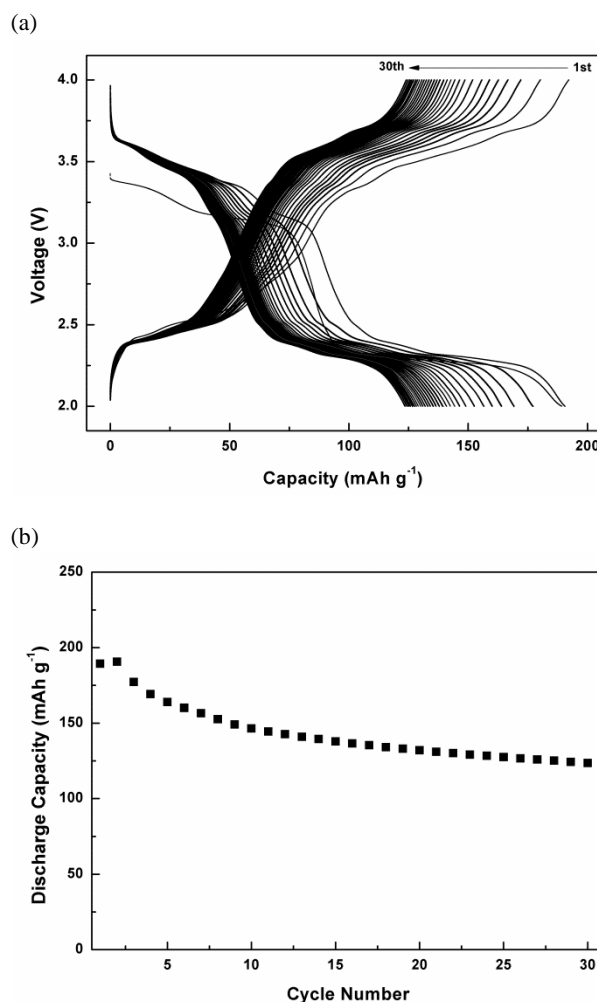


Fig. 10 (a) Charge/discharge curves and (b) discharge capacity profiles of all-solid-state Li/BCP21/ V_2O_5 cell cycled at 60 °C (0.1C).

high initial discharge capacity of 190 mAh g^{-1} was observed, while it continuously decreases and stabilizes to 124 mAh g^{-1} , resulting in 65 % of capacity retention after 30 cycles. The relatively low capacity retention behavior might be caused by the solid nature of SPEs because the possible interfacial resistance between the interface of solid electrolyte and the cathode can prevent the full utilization of active materials in cathode.⁷² However, this result still demonstrates that BCP21 has possibility to be used in high-temperature lithium-ion battery system without causing safety problems. Also, further experiments to enhance the capacity value as well as their retention by optimizing the composition of cathode materials and electrode coating method by changing the polymeric binder materials are under carrying out.

Conclusions

Organic/inorganic hybrid branched-graft copolymers (BCPs) containing PEGMA and MA-POSS moieties were synthesized by simple one-step RAFT polymerization. Linear-graft

copolymers (LCPs) with PEGMA and MA-POSS moieties were also synthesized for comparison. Enhanced ionic conductivities and dimensional stability of the SPEs were accomplished by controlling the polymer structures and the MA-POSS content in the copolymers. Maximum ionic conductivity of 1.6×10^{-4} S/cm at 60 °C was achieved for the BCP21 electrolyte containing 21 mol % of MA-POSS and 79 mol % of PEGMA moieties. It is very worthy to note that the MA-POSS moieties maintain the chain mobility of polymers despite its own rigidity as well as provide significant dimensional stability to the SPEs even at the high temperature. The branched-graft BCP21 electrolyte exhibited higher ionic conductivity than the linear-graft LCP21 electrolyte because the branched structure gives larger chain mobility to the polymers as estimated by the lower T_g value of ion-conducting segments. BCP21 exhibits wide electrochemically stable potential window and all-solid-state battery test at 60 °C was successfully performed without causing safety problem. All of these unique features of BCPs suggest that the SPEs with branched structure containing POSS moieties are very promising candidate for the field of high-temperature lithium-ion battery applications.

Acknowledgements

This research was supported by the Technology Innovation Program (grant number: 10045221) funded by the Ministry of Trade, Industry and Energy (MOTIE, Korea).

Notes and references

School of Chemical and Biological Engineering and Institute of Chemical Processes, Seoul National University, 599 Gwanak-ro, Gwanak-gu, Seoul 151-742, Republic of Korea. Fax: +82-02-880-8899; Tel: +82-02-880-7070; E-mail: jongchan@snu.ac.kr

- A. Manuel Stephan and K. S. Nahm, *Polymer*, 2006, **47**, 5952-5964.
- W. H. Meyer, *Adv. Mater.*, 1998, **10**, 439-448.
- J. M. Tarascon and M. Armand, *Nature*, 2001, **414**, 359-367.
- D. E. Fenton, J. M. Parker and P. V. Wright, *Polymer*, 1973, **14**, 589-589.
- Q. Li, H. Y. Sun, Y. Takeda, N. Imanishi, J. Yang and O. Yamamoto, *J. Power Sources*, 2001, **94**, 201-205.
- M. S. Michael, M. M. E. Jacob, S. R. S. Prabaharan and S. Radhakrishna, *Solid State Ionics*, 1997, **98**, 167-174.
- Y. T. Shieh, G. L. Liu, K. C. Hwang and C. C. Chen, *Polymer*, 2005, **46**, 10945-10951.
- S. J. Park, A. R. Han, J. S. Shin and S. Kim, *Macromol. Res.*, 2010, **18**, 336-340.
- X. H. Flora, M. Ulaganathan, R. Babu and S. Rajendran, *Ionics*, 2012, **18**, 731-736.
- H. J. Ha, E. H. Kil, Y. H. Kwon, J. Y. Kim, C. K. Lee and S. Y. Lee, *Energ. Environ. Sci.*, 2012, **5**, 6491-6499.
- Y. Kato, S. Yokoyama, H. Ikuta, Y. Uchimoto and M. Wakihara, *Electrochem. Commun.*, 2001, **3**, 128-130.
- N. A. A. Rossi, Z. Zhang, Y. Schneider, K. Morcom, L. J. Lyons, Q. Wang, K. Amine and R. West, *Chem. Mater.*, 2006, **18**, 1289-1295.
- L. Zhang, Z. Zhang, S. Harring, M. Straughan, R. Butorac, Z. Chen, L. Lyons, K. Amine and R. West, *J. Mater. Chem.*, 2008, **18**, 3713-3717.
- J. Y. Ji, J. Keen and W. H. Zhong, *J. Power Sources*, 2011, **196**, 10163-10168.
- S.-K. Kim, D.-G. Kim, A. Lee, H.-S. Sohn, J. J. Wie, N. A. Nguyen, M. E. Mackay and J.-C. Lee, *Macromolecules*, 2012, **45**, 9347-9356.
- P. P. Soo, B. Y. Huang, Y. I. Jang, Y. M. Chiang, D. R. Sadoway and A. M. Mayes, *J. Electrochem. Soc.*, 1999, **146**, 32-37.
- D. He, S. Y. Cho, D. W. Kim, C. Lee and Y. Kang, *Macromolecules*, 2012, **45**, 7931-7938.
- B. Oh, D. Vissers, Z. Zhang, R. West, H. Tsukamoto and K. Amine, *J. Power Sources*, 2003, **119-121**, 442-447.
- J. L. Nugent, S. S. Moganty and L. A. Archer, *Adv. Mater.*, 2010, **22**, 3677-3680.
- F. Wang, X. Lu and C. He, *J. Mater. Chem.*, 2011, **21**, 2775-2782.
- B. H. Tan, H. Hussain, Y. W. Leong, T. T. Lin, W. W. Tjiu and C. B. He, *Polym. Chem.*, 2013, **4**, 1250-1259.
- J. Pyun and K. Matyjaszewski, *Macromolecules*, 2000, **33**, 217-220.
- A. Strachota, I. Kroutilová, J. Kovářová and L. Matějka, *Macromolecules*, 2004, **37**, 9457-9464.
- J. Wu, T. S. Haddad and P. T. Mather, *Macromolecules*, 2009, **42**, 1142-1152.
- H.-S. Ryu, D.-G. Kim and J.-C. Lee, *Macromol. Res.*, 2010, **18**, 1021-1029.
- H.-S. Ryu, D.-G. Kim and J.-C. Lee, *Polymer*, 2010, **51**, 2296-2304.
- D.-G. Kim, H.-S. Sohn, S.-K. Kim, A. Lee and J.-C. Lee, *J. Polym. Sci., Part A: Polym. Chem.*, 2012, **50**, 3618-3627.
- H. J. Zhang, S. Kulkarni and S. L. Wunder, *J. Phys. Chem. B*, 2007, **111**, 3583-3590.
- H. J. Zhang, S. Kulkarni and S. L. Wunder, *J. Electrochem. Soc.*, 2006, **153**, A239-A248.
- C. J. Hawker, F. K. Chu, P. J. Pomery and D. J. T. Hill, *Macromolecules*, 1996, **29**, 3831-3838.
- T. Itoh, Y. Ichikawa, N. Hirata, T. Uno, M. Kubo and O. Yamamoto, *Solid State Ionics*, 2002, **150**, 337-345.
- T. Uno, H. Sano, M. Matsumoto, M. Kubo and T. Itoh, *J. Solid State Electr.*, 2010, **14**, 2161-2167.
- D. Wilms, M. Schomer, F. Wurm, M. I. Hermanns, C. J. Kirkpatrick and H. Frey, *Macromol. Rapid Commun.*, 2010, **31**, 1811-1815.
- M. Marzantowicz, J. R. Dygas, F. Krok, A. Tomaszewska, Z. Florjanczyk, E. Zygadlo-Monikowska and G. Lapienis, *J. Power Sources*, 2009, **194**, 51-57.
- P. A. Costello, I. K. Martin, A. T. Slark, D. C. Sherrington and A. Titterton, *Polymer*, 2002, **43**, 245-254.
- H. R. Allcock, S. J. M. O'Connor, D. L. Olmeijer, M. E. Napierala and C. G. Cameron, *Macromolecules*, 1996, **29**, 7544-7552.
- T. Itoh, S. Gotoh, S. Horii, S. Hashimoto, T. Uno, M. Kubo, T. Fujinami and O. Yamamoto, *J. Power Sources*, 2005, **146**, 371-375.
- T. Itoh, S. Horii, T. Uno, M. Kubo and O. Yamamoto, *Electrochim. Acta*, 2004, **50**, 271-274.
- Y. Lin, F. Zeng-Guo, Z. Yu-Mei, W. Feng, C. Shi and W. Guo-Qing, *J. Polym. Sci., Part A: Polym. Chem.*, 2006, **44**, 3650-3665.
- Z. X. Wang, M. Ikeda, N. Hirata, M. Kubo, T. Itoh and O. Yamamoto, *J. Electrochem. Soc.*, 1999, **146**, 2209-2215.
- Z. Wen, T. Itoh, M. Ikeda, N. Hirata, M. Kubo and O. Yamamoto, *J. Power Sources*, 2000, **90**, 20-26.

- 42 M. Benaglia, E. Rizzardo, A. Alberti and M. Guerra, *Macromolecules*, 2005, **38**, 3129-3140.
- 43 H. S. Sohn, S. H. Cha, W. K. Lee, D. G. Kim, H. J. Yun, M. S. Kim, B. D. Kim, Y. H. Kim, J. W. Lee, J. S. Kim, D. B. Kim, J. H. Kim and J. C. Lee, *Macromol. Res.*, 2011, **19**, 722-728.
- 44 J. Zhu, X. L. Zhu, Z. P. Cheng, F. Liu and J. M. Lu, *Polymer*, 2002, **43**, 7037-7042.
- 45 M. Dietrich, M. Glassner, T. Gruending, C. Schmid, J. Falkenhagen and C. Barner-Kowollik, *Polym. Chem.*, 2010, **1**, 634-644.
- 46 X. Y. Jiang, Y. J. Li, G. L. Lu and X. Y. Huang, *Polym. Chem.*, 2013, **4**, 1402-1411.
- 47 C. P. Li, J. Q. Wang, Y. Shi, Z. Liu, J. Lin and Z. F. Fu, *Macromol. Res.*, 2012, **20**, 858-867.
- 48 R. Severac, P. Lacroix-Desmazes and B. Boutevin, *Polym. Int.*, 2002, **51**, 1117-1122.
- 49 M. Wang, L. Qi, F. Zhao and S. Dong, *J. Power Sources*, 2005, **139**, 223-229.
- 50 B. L. Liu, A. Kazlauciusas, J. T. Guthrie and S. Perrier, *Macromolecules*, 2005, **38**, 2131-2136.
- 51 Y. Lin, X. Liu, X. Li, J. Zhan and Y. Li, *J. Polym. Sci., Part A: Polym. Chem.*, 2007, **45**, 26-40.
- 52 J. Chiefari, Y. K. Chong, F. Ercole, J. Krstina, J. Jeffery, T. P. T. Le, R. T. A. Mayadunne, G. F. Meijs, C. L. Moad, G. Moad, E. Rizzardo and S. H. Thang, *Macromolecules*, 1998, **31**, 5559-5562.
- 53 H. Hussain, B. H. Tan, G. L. Seah, Y. Liu, C. B. He and T. P. Davis, *Langmuir*, 2010, **26**, 11763-11773.
- 54 D. Yan, W. J. Wang and S. Zhu, *Polymer*, 1999, **40**, 1737-1744.
- 55 P. R. Chinnam and S. L. Wunder, *Chem. Mater.*, 2011, **23**, 5111-5121.
- 56 J. K. H. Teo, C. L. Toh and X. H. Lu, *Polymer*, 2011, **52**, 1975-1982.
- 57 J. Wu, T. S. Haddad, G. M. Kim and P. T. Mather, *Macromolecules*, 2007, **40**, 544-554.
- 58 S. Guns, P. Kayaert, J. A. Martens, J. Van Humbeeck, V. Mathot, T. Pijpers, E. Zhuravlev, C. Schick and G. Van den Mooter, *Eur. J. Pharm. Biopharm.*, 2010, **74**, 239-247.
- 59 J.-C. Lee, M. H. Litt and C. E. Rogers, *J. Polym. Sci., Part A: Polym. Chem.*, 1998, **36**, 495-504.
- 60 J.-W. Rhim, H. B. Park, C.-S. Lee, J.-H. Jun, D. S. Kim and Y. M. Lee, *J. Membrane Sci.*, 2004, **238**, 143-151.
- 61 S. Roy, J. Feng, V. Scionti, S. C. Jana and C. Wesdemiotis, *Polymer*, 2012, **53**, 1711-1724.
- 62 R. Verker, E. Grossman, I. Gouzman and N. Eliaz, *Compos. Sci. Technol.*, 2009, **69**, 2178-2184.
- 63 H. Rios-Dominguez, F. A. Ruiz-Trevino, R. Contreras-Reyes and A. Gonzalez-Montiel, *J. Membrane Sci.*, 2006, **271**, 94-100.
- 64 T. Hirai, M. Leolukman, C. C. Liu, E. Han, Y. J. Kim, Y. Ishida, T. Hayakawa, M.-a. Kakimoto, P. F. Nealey and P. Gopalan, *Adv. Mater.*, 2009, **21**, 4334-4338.
- 65 G. Z. Li, L. Wang, H. Toghiani, T. L. Daulton and C. U. Pittman, *Polymer*, 2002, **43**, 4167-4176.
- 66 F. Zhao, X. Bao, A. R. McLauchlin, J. Gu, C. Wan and B. Kandasubramanian, *Appl. Clay Sci.*, 2010, **47**, 249-256.
- 67 H. Y. Wu, D. Saikia, C. P. Lin, F. S. Wu, G. T. K. Fey and H. M. Kao, *Polymer*, 2010, **51**, 4351-4361.
- 68 I. Albinsson, B. E. Mellander and J. R. Stevens, *Solid State Ionics*, 1993, **60**, 63-66.
- 69 M. Watanabe, Y. Suzuki and A. Nishimoto, *Electrochim. Acta*, 2000, **45**, 1187-1192.
- 70 D. K. Lee and H. R. Allcock, *Solid State Ionics*, 2010, **181**, 1721-1726.
- 71 P. G. Bruce and C. A. Vincent, *J. Chem. Soc. Faraday T*, 1993, **89**, 3187-3203.
- 72 M. Nakayama, S. Wada, S. Kuroki and M. Nogami, *Energ. Environ. Sci.*, 2010, **3**, 1995-2002.